Receive Antenna Selection for Time-Varying Channels Using Discrete Prolate Spheroidal Sequences

Hassan A. Abou Saleh, *Student Member, IEEE,* Andreas F. Molisch, *Fellow, IEEE,* Thomas Zemen, *Senior Member, IEEE,* Steven D. Blostein, *Senior Member, IEEE,* and Neelesh B. Mehta, *Senior Member, IEEE*

***Abstract*—Receive antenna selection (AS) has been shown to maintain the diversity benefits of multiple antennas while potentially reducing hardware costs. However, the promised diversity gains of receive AS depend on the assumptions of perfect channel knowledge at the receiver and slowly time-varying fading. By explicitly accounting for practical constraints imposed by the next-generation wireless standards such as training, packetization and antenna switching time, we propose a single receive AS method for time-varying fading channels. The method exploits the low training overhead and accuracy possible from the use of discrete prolate spheroidal (DPS) sequences based reduced rank subspace projection techniques. It only requires knowledge of the Doppler bandwidth, and does not require detailed correlation knowledge. Closed-form expressions for the channel prediction and estimation error as well as symbol error probability (SEP) of M-ary phase-shift keying (MPSK) for symbol-by-symbol receive AS are also derived. It is shown that the proposed AS scheme, after accounting for the practical limitations mentioned above, outperforms the ideal conventional single-input single-output (SISO) system with perfect CSI and no AS at the receiver and AS with conventional estimation based on complex exponential basis functions.**

***Index Terms*—Antenna selection, time-varying fading, discrete prolate spheroidal sequences, Slepian basis expansion.**

I. Introduction

To accommodate the rate and reliability requirements set by forthcoming applications such as wireless broadband access and mobile television, next-generation wireless standards such as IEEE 802.11n [1] and long term evolution (LTE) of the third generation partnership project (3GPP) [2] have adopted multiple-input multiple-output (MIMO) technology, orthogonal frequency division multiplexing (OFDM) and/or orthogonal frequency division multiple access (OFDMA) as signalling formats over the physical channel. Further, AS at the transmitter and/or receiver has been standardized, e.g., in IEEE 802.11n, or is being standardized [3].

Antenna selection may be used to reduce hardware complexity at the transmitter and/or receiver of a wireless system. In AS, only a subset of the antenna elements (AEs) is connected to a limited number of radio-frequency (RF) chains based on the current channel fades. This potentially retains the advantages of multiple antennas, despite using fewer of the expensive RF chains that are comprised of low-noise amplifiers (LNAs), mixers, and oscillators [4], [5]. We focus here on the practical single receive AS scenario because it retains most of the diversity benefits of multiple antennas while minimizing hardware complexity. As will be shown, performance evaluation of even the single AS problem is very challenging.

There are a number of existing studies on both optimal and suboptimal AS algorithms [6], [7] as well as on the capacity, diversity, and diversity-multiplexing (D-M) performance of AS [8]–[13]. However, to date, far fewer studies exist that deal with the practical issues of pilot-based training and AS implementation. A media-access-control (MAC) based AS training and calibration protocol, in which the AEs are trained using packets transmitted in burst mode is proposed in [14] for slowly time-varying environments. The protocol in [14] is adopted in the IEEE 802.11n standard for high-throughput wireless local area networks (WLANs).

In the above references, perfect channel knowledge is assumed. However, the mobile communication environment exhibits a randomly time-varying channel due to the mobility of users and reflections from multiple scatterers. This implies that channel state information (CSI) gets rapidly outdated, limiting the accuracy of the channel knowledge at the receiver. The impact of erroneous CSI on the performance of a space-time coded AS system in Rayleigh fading is studied in [15]. The performance of maximal ratio transmission (MRT) and transmit antenna selection with space-time block coding (TAS/STBC) in MIMO systems with both CSI feedback delay and channel estimation error is analyzed in [16]. An analytical framework to evaluate the symbol error probability (SEP) performance for diversity systems in which a subset of the available diversity branches are selected and combined

Manuscript received August 23, 2011; revised December 21, 2011; accepted March 27, 2012. The associate editor coordinating the review of this paper and approving it for publication is G. Abreu.

This paper was presented in part at the IEEE International Conference on Communications, Ottawa, ON, Canada, June 2012.

H. A. Saleh and S. D. Blostein are with the Dept. of Electrical and Computer Eng., Queen's University, Kingston, ON, Canada (e-mail: hassan.abou.saleh@ieee.org, steven.blostein@queensu.ca).

A. F. Molisch is with the Dept. of Electrical Eng., University of Southern California (USC), Los Angeles, CA, USA (e-mail: molisch@usc.edu).

T. Zemen is with FTW Forschungszentrum Telekommunikation Wien (Telecommunications Research Center Vienna), Vienna, Austria (e-mail: thomas.zemen@ftw.at).

N. B. Mehta is with the Dept. of Electrical and Communication Eng., Indian Institute of Science (IISc), Bangalore, India (e-mail: nbmehta@ece.iisc.ernet.in).

Digital Object Identifier 10.1109/TWC.2012.050112.111582

over flat Rayleigh fading with imperfect channel knowledge is developed in [17]. Receive AS for space-time-frequency (STF) coded MIMO-OFDM systems with imperfect channel estimation is studied in [18]. The effects of feedback delay and channel estimation errors on the performance of a MIMO system employing AS at the transmitter and maximal ratio combining (MRC) at the receiver is studied in [19]. In [19], it is shown that channel estimation errors result in a fixed signal-to-noise ratio (SNR) loss while feedback delay alters the diversity order.

Motivated by the fact that AE channel gain estimates are outdated by different amounts in time-varying channels, a single-antenna selection rule is proposed in [20] which minimizes the SEP of M-ary PSK (MPSK)/MQAM by linearly weighting the channel estimates before selection. In [20], it is shown that the optimal weights are proportional to the temporal channel correlation coefficients of the antennas. The general case of selecting more than one antenna and the problem of *training voids* have been recently treated in [21]. However, it is worth mentioning that only channel gain estimates obtained during the *AS training phase* are used in the selection and decoding mechanisms in [20] and [21] since channel gain estimates over the *data transmission phase* are not available, which incurs a loss in SNR. We also note that the weighted selection criterion used in [20] and [21] requires temporal correlation knowledge.

The above observations motivate investigation into practical training-based AS algorithms for time-varying channels which use channel knowledge in the data transmission phase in the selection and decoding processes by utilizing channel prediction. It is important to highlight that the optimal Wiener predictor utilizes detailed covariance knowledge, which is difficult to obtain due to bursty transmission, or over the short time interval in which the channel is wide-sense stationary in vehicular scenarios [22]. This motivates the use of the recently-proposed low-complexity Slepian basis expansion channel estimator [23] and channel predictor [22] to obtain reliable CSI at the receiver. This Slepian basis expansion estimator/predictor uses discrete prolate spheroidal (DPS) sequences as basis functions which enables low-complexity reduced-rank channel estimation/prediction. Furthermore, in contrast to many linear estimation/prediction techniques that require detailed autocorrelation knowledge, it requires only knowledge of the Doppler bandwidth. In [23], the Slepian basis expansion channel estimator is used to estimate the time-varying channel for each subcarrier of a multiuser multi-carrier code division multiple access (MC-CDMA) system. It is shown that with a pilot-to-packet length ratio of only 2%, the bit error rate (BER) of the system approaches that of a system with perfect CSI. It is shown in [22] that for a prediction horizon of one eighth of a wavelength, the Slepian basis expansion channel predictor outperforms the classical predictor that uses complex exponentials as the basis. We note that the complex exponential predictor utilizes the exact Doppler frequencies of each propagation path of the channel. For a prediction horizon of three eighths of a wavelength, the performance of the Slepian basis expansion channel predictor is shown to be very close to that of the optimal Wiener predictor.

In this paper, we propose and analyze the performance of a training-based single receive AS system in time-varying channels that uses the Slepian basis expansion predictor and estimator. The paper's contributions are summarized as follows:

- A method for accurately estimating/predicting time-varying frequency-flat channels, which utilizes projections onto a subspace spanned by orthonormal DPS sequences [22], [23], is extended to AS.
- Closed-form expressions are provided for the channel prediction and estimation error as well as the SEP of MPSK with receive AS, and verified with Monte Carlo simulation results.
- Extensive simulation results are presented to compare the performance of the proposed AS method with ideal conventional single-input single-output (SISO) systems with perfect CSI but no AS at the receiver and AS based on prediction/estimation techniques that are based on complex exponential basis functions.

The paper is organized as follows: the detailed system model is described in Sec. II, and the Slepian basis expansion predictor and estimator are then introduced in Sec. III. The training-based receive AS method is described in Sec. IV. The SEP is analyzed in Sec. V. Analytical and simulation results are discussed in Sec. VI. Our conclusions follow in Sec. VII. Detailed mathematical derivations are provided in the Appendix.

II. System Model

Consider the downlink of a cellular radio system consisting of a single-antenna base station (BS) transmitting to a K-antenna element (AE) mobile station (MS) equipped with only one RF chain as depicted in Fig. 1. A micro-electromechanical system (MEMS) based antenna switch connects the selected AE to the RF chain; such switches provide sufficient switching speeds while keeping the insertion loss in the order of 0.1 dB, which is negligible.

Each AS cycle consists of an *AS training phase* followed by a *data transmission phase*, as illustrated in Fig. 2. We first introduce DPS sequences which are used to predict/estimate the time-varying channel over the data transmission phase as shown in Sec. III, and then describe the AS training and data transmission phases.

A. Discrete Prolate Spheroidal (DPS) Sequences

The orthogonal DPS sequences are simultaneously band-limited to the frequency range $\mathcal{W} = (-\nu_{\max}, +\nu_{\max})$ and energy-concentrated in the time interval $\mathcal{I}_{\text{bl}} = \{0, 1, \ldots, M'-1\}$, where the normalized one-sided Doppler bandwidth $\nu_{\max}$ is given by

$$\nu_{\max} \triangleq \frac{v_{\max} f_{\text{c}}}{c} T_{\text{s}} \ll \frac{1}{2} \tag{1}$$

where $v_{\max}$ is the radial component of the user velocity, f_{c} is the carrier frequency, and c is the speed of light. The M' DPS sequences $\{u_i[m] \mid m \in \mathbb{Z}\}_{i=0}^{M'-1}$ are defined as the real

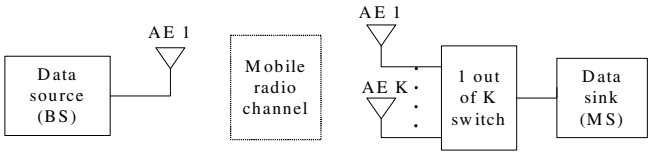

Fig. 1. Antenna selection system model.

solutions to the following system of linear equations [23]

$$\sum_{l=0}^{M'-1} C\left[l-m\right]\, u_i\left[l\right] = \lambda_i\, u_i\left[m\right], \qquad m \in \mathbb{Z},\ i \in \mathcal{I}_{\text{bl}} \tag{2}$$

where

$$C\left[l-m\right] = \frac{\sin\left(2\pi\nu_{\max}\left(l-m\right)\right)}{\pi\left(l-m\right)}. \tag{3}$$

The eigenvalues $\{\lambda_i\}_{i=0}^{M'-1}$ decay exponentially for $i \geq D'$, where the essential subspace dimension D' is given by [23]

$$D' = \lceil 2\,\nu_{\max}\,M' \rceil + 1 \tag{4}$$

and $\lceil x \rceil$ denotes the smallest integer greater than or equal to x.

As mentioned earlier, the DPS sequences $\{u_i\left[m\right] \mid m \in \mathbb{Z}\}_{i=0}^{M'-1}$ are orthogonal. Further, even the restrictions of the DPS sequences on $\mathcal{I}_{\text{bl}}$, i.e., $\{u_i\left[m\right] \mid m \in \mathcal{I}_{\text{bl}}\}_{i=0}^{M'-1}$, are orthonormal [23], and, thus, form a set of M'-length basis vectors $\{\boldsymbol{u}_i\}_{i=0}^{M'-1}$. Based on (2), the length-M' basis vectors $\{\boldsymbol{u}_i\}_{i=0}^{M'-1}$ are, thus, the eigenvectors of the $M' \times M'$ matrix $\boldsymbol{C}$ [23]

$$\boldsymbol{C}\,\boldsymbol{u}_i = \lambda_i\,\boldsymbol{u}_i \tag{5}$$

where $M' \times 1$ basis vector $\boldsymbol{u}_i \triangleq \left[u_i\left[0\right], u_i\left[1\right], \ldots, u_i\left[M'-1\right]\right]^T$ with $(\cdot)^T$ denoting the transpose. The entries of $\boldsymbol{C}$ are formed from (3) as $[\boldsymbol{C}]_{l,m} = C\left[l-m\right]$ for $l,\ m \in \mathcal{I}_{\text{bl}}$. As shown in Sec. III-A, the DPS sequences time-limited to $\mathcal{I}_{\text{bl}}$, which form an orthonormal set of basis functions $\{\boldsymbol{u}_i\}_{i=0}^{M'-1}$, can be used to estimate the time-varying channel over $\mathcal{I}_{\text{bl}}$.

B. AS Training Phase

In each *AS training phase*, the BS transmits $L \geq 2$ training symbols sequentially in time to each antenna. We note here that more than one pilot symbol is needed in order to employ AS in time-varying channels to improve channel prediction. Pilot symbols are used to estimate the predictor's basis expansion coefficients as discussed in Sec. III. We also note that the 3GPP-LTE standard uses two training symbols within a 1 ms duration to improve channel estimation. The duration between consecutive pilots for AE k and AE $k+1$ is $T_{\text{p}} \triangleq \alpha\, T_{\text{s}}$, where T_{s} is the symbol duration and $\alpha \geq 2$. Two consecutive AS training pilots transmitted for each AE are thus separated in time by a duration of $T_{\text{t}} \triangleq K\,T_{\text{p}} = \alpha\,K\,T_{\text{s}}$. The pilot and data symbol duration T_{s} is assumed to be much longer than the delay spread and much shorter than the coherence time of the channel, i.e., the channel is frequency-flat time-varying. The data symbols are drawn with equal probability from an MPSK constellation of average energy $E_{\text{s}} = 1$.

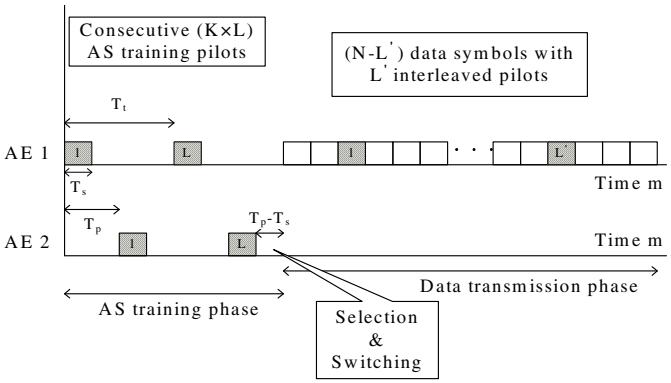

Fig. 2. Antenna selection cycle consists of AS training and data transmission phases. (AE 1 is selected, $K = 2$, $L = 2$, $L' = 2$, and $T_{\text{p}} = 2\,T_{\text{s}}$).

Let m index discrete time with sampling rate $R_{\text{s}} \triangleq \frac{1}{T_{\text{s}}}$. The channel gain $h_k\left[m\right]$ is estimated from the AS training pilot symbol $p_k\left[m\right]$ that is received by AE k at time $m \in T_{\text{tr}}^k$. The received signal is

$$y_k\left[m\right] = h_k\left[m\right]\, p_k\left[m\right] + n_k\left[m\right], \qquad 1 \leq k \leq K,\ m \in T_{\text{tr}}^k \tag{6}$$

where

$$T_{\text{tr}}^k \triangleq \{\alpha\,\left[(k-1) + K\,\left(\ell-1\right)\right]\}, \qquad 1 \leq \ell \leq L \tag{7}$$

denotes the set of time indices when the L AS training pilots are received by AE k, $h_k\left[m\right]$ is the sampled time-varying channel gain, and $n_k\left[m\right]$ is additive white Gaussian noise (AWGN) with variance N_0 and is independent of $h_k\left[m\right]$. Based on (6), channel gain estimates $\left\{\tilde{h}_k\left[m\right] \mid m \in T_{\text{tr}}^k\right\}$ for AE k can be expressed as

$$\begin{aligned}\tilde{h}_k\left[m\right] &= y_k\left[m\right]\, p_k^*\left[m\right] \\ &\triangleq h_k\left[m\right] + e_k^{\text{n}}\left[m\right], \quad 1 \leq k \leq K,\ m \in T_{\text{tr}}^k\end{aligned} \tag{8}$$

where $(\cdot)^*$ denotes complex conjugate and $e_k^{\text{n}}\left[m\right] \triangleq n_k\left[m\right]\, p_k^*\left[m\right]$ is the channel estimation error resulting from the AWGN. From (7) and accounting for the additional selection and switching time of duration $T_{\text{p}} - T_{\text{s}}$, it follows that the *AS training phase* spans the discrete time interval $\mathcal{I}_{\text{tr}} = \{0, 1, \ldots, M-1\}$, where $M = \alpha\,K\,L$.

Using the noisy channel estimates $\left\{\tilde{h}_k\left[m\right] \mid m \in T_{\text{tr}}^k\right\}$, the receiver performs minimum-energy (ME) band-limited channel prediction [22] for each antenna over the *data transmission phase* time interval $\mathcal{I}_{\text{dt}} = \{M, M+1, \ldots, M+N-1\}$. Denote the predicted channel gains by $\left\{\hat{h}_k^{\text{SP}}\left[m\right] \mid m \in \mathcal{I}_{\text{dt}}\right\}$, where the superscript $(\cdot)^{\text{SP}}$ indicates Slepian prediction [22]. The MS selects its receive antenna according to a certain criterion, and then switches its RF chain accordingly.

Depending on the AS switching time, either per-packet or symbol-by-symbol AS can be used. For example, solid-state switches achieve switching times on the order of hundreds of nanoseconds, which is less than typical cyclic prefixes, and thus enable the switching of antennas between symbols. Thus, different symbols of a packet may be received by their

most suitable AEs as the channel varies with time. However, these switches have attenuations on the order of 1 to 3 dB. In contrast, MEMS switches have attenuations on the order of 0.1 to 0.3 dB, but achieve switching times on the order of microseconds, and thus typically enable only per-packet switching. We note as the AS switching times and attenuations decrease, symbol-by-symbol switching may become viable in futuristic systems. Furthermore, similar to 802.11n, per-packet switching can be enabled by modifications of the MAC layer, while per-symbol switching requires changes to the physical-layer standard. Therefore, both symbol-by-symbol and per-packet switching are relevant, and are both considered in our analysis. We denote by $\hat{\imath}$ the index of the selected antenna, with $\hat{(\cdot)}$ indicating that the selection is based on (imperfect) prediction and/or estimation.

C. Data Transmission Phase

In each *data transmission phase* the BS sends out a length-N data packet, which consists of $N-L'$ data symbols and L' interleaved post-selection pilot symbols. The symbol locations in the packet that carry the pilots are given by [23]

$$\mathcal{P} \triangleq \left\{ \left\lfloor (\ell'-1)\ \frac{N}{L'} + \frac{N}{2\,L'} \right\rfloor \ \middle|\ 1 \le \ell' \le L' \right\} \tag{9}$$

where $\lfloor x \rfloor$ denotes the largest integer not greater than x. After selection, the pilots are received by AE $\hat{\imath}$ at times $m \in T_{\text{dt}}$, where

$$T_{\text{dt}} \triangleq \left\{ M-1+\left\lfloor (\ell'-1)\ \frac{N}{L'} + \frac{N}{2\,L'} \right\rfloor \ \middle|\ 1 \le \ell' \le L' \right\} \tag{10}$$

and $M = \alpha\, K\, L$. Thus, in total, $L_{\text{tot}} \triangleq L + L'$ pilot symbols are received by AE $\hat{\imath}$ at times $m \in T_{\text{tot}}^{\hat{\imath}}$, where

$$T_{\text{tot}}^{\hat{\imath}} = T_{\text{tr}}^{\hat{\imath}} \cup T_{\text{dt}} \tag{11}$$

with $T_{\text{tr}}^{\hat{\imath}}$ and T_{dt} given in (7) and (10), respectively. From these L_{tot} pilots, refined channel gain estimates $\left\{ \hat{h}_{\hat{\imath}}^{\text{SE}}[m] \mid m \in \mathcal{I}_{\text{dt}} \right\}$ of the selected AE $\hat{\imath}$ are obtained using the Slepian basis expansion channel estimator [23] and used to decode data. The received signal at AE $\hat{\imath}$ can be expressed as

$$y_{\hat{\imath}}[m] = h_{\hat{\imath}}[m]\ s[m] + n_{\hat{\imath}}[m], \qquad m \in \mathcal{I}_{\text{dt}} \tag{12}$$

where the transmitted symbol $s[m]$ is given by

$$s[m] = \begin{cases} d[m], & m \in \mathcal{I}_{\text{dt}} \backslash T_{\text{dt}} \\ p[m], & m \in T_{\text{dt}} \end{cases}. \tag{13}$$

Here, $d[m]$ and $p[m]$ denote the transmitted data and post-selection pilot symbols, respectively.

III. Reduced-rank channel estimation and minimum-energy band-limited prediction

A. Reduced-Rank Channel Estimation

To enable estimation of a time-varying channel for a length-M' block of data transmission, $M'-J$ data symbols and J interleaved pilot symbols are transmitted in a pattern specified by index set $\mathcal{J}$.

The aforementioned DPS sequences time-limited to $\mathcal{I}_{\text{bl}} = \{0, 1, \ldots, M'-1\}$ are used to estimate the time-varying channel over time interval $\mathcal{I}_{\text{bl}}$. The basis expansion estimator approximates the $M' \times 1$ true channel vector $\boldsymbol{h} \triangleq \left[h[0], h[1], \ldots, h[M'-1]\right]^T$ in terms of a linear combination $\hat{\boldsymbol{h}}^{\text{SE}}$ of D length-M' basis vectors $\{\boldsymbol{u}_i\}_{i=0}^{D-1}$ as [22]

$$\boldsymbol{h} \approx \hat{\boldsymbol{h}}^{\text{SE}} = \boldsymbol{U}\,\hat{\boldsymbol{\gamma}} = \sum_{i=0}^{D-1} \hat{\gamma}_i\, \boldsymbol{u}_i \tag{14}$$

where $\boldsymbol{U} \triangleq \left[\boldsymbol{u}_0, \ldots, \boldsymbol{u}_{D-1}\right]$ is an $M' \times D$ matrix, $\boldsymbol{u}_i \triangleq \left[u_i[0], u_i[1], \ldots, u_i[M'-1]\right]^T$, and D is the optimal subspace dimension which minimizes the mean-square-error (MSE) in the above approximation. It is given by

$$D = \underset{d\,\in\,\{1,\ldots,J\}}{\operatorname{argmin}} \left(\frac{1}{2\,\nu_{\max}\,J} \sum_{i=d}^{J-1} \lambda_i + \frac{d}{J}\,N_0 \right) \tag{15}$$

where $\eta \triangleq \frac{E_s}{N_0}$ is the average SNR. In (15), the eigenvalues are assumed to be ranked as $\lambda_0 \ge \lambda_1 \ge \ldots \ge \lambda_{J-1}$. The $D \times 1$ vector $\hat{\boldsymbol{\gamma}} \triangleq \left[\hat{\gamma}_0, \hat{\gamma}_1, \ldots, \hat{\gamma}_{D-1}\right]^T$ contains the basis expansion coefficients. It is estimated using the J interleaved pilot symbols $\{p[l] \mid l \in \mathcal{J}\}$, received at times $l \in \mathcal{J}$, via [23]

$$\hat{\boldsymbol{\gamma}} = \boldsymbol{G}^{-1} \sum_{l\in\mathcal{J}} y[l]\ p^*[l]\ \boldsymbol{f}^*[l] \tag{16}$$

where $y[l]$ is the received signal, the $D \times 1$ vector $\boldsymbol{f}[l]$ is defined as $\left[u_0[l], \ldots, u_{D-1}[l]\right]^T$, and $\boldsymbol{G}$ is a $D \times D$ matrix given by

$$\boldsymbol{G} = \sum_{l\in\mathcal{J}} \boldsymbol{f}\ [l]\ \boldsymbol{f}^{\dagger}[l] \tag{17}$$

where $(\cdot)^{\dagger}$ denotes Hermitian transpose.

B. Minimum-Energy Band-Limited Channel Prediction

The ME band-limited predictor uses the extension of the DPS sequences that are time-limited to $\mathcal{I}_{\text{bl}}$ as the basis vectors. They are calculated by [22]

$$u_i[m] = \frac{1}{\lambda_i} \sum_{l=0}^{M'-1} C[l-m]\ u_i[l], \qquad m \in \mathbb{Z} \setminus \mathcal{I}_{\text{bl}}. \tag{18}$$

The ME band-limited prediction of a time-varying frequency-flat channel can be expressed as [22]

$$\hat{h}^{\text{SP}}[m] = \boldsymbol{f}^T[m]\ \hat{\boldsymbol{\gamma}} = \sum_{i=0}^{D-1} \hat{\gamma}_i\, u_i[m], \qquad m \in \mathbb{Z} \setminus \mathcal{I}_{\text{bl}} \tag{19}$$

where $\boldsymbol{f}[m] = [u_0[m], \ldots, u_{D-1}[m]]^T$.

IV. Downlink Receive Antenna Selection Algorithm

We propose the following training-based "one out of K" receive AS algorithm for time-varying channels for per-packet switching:

1) Following an AS request, each AE is trained using $L \ge 2$ pilot symbols. The spacing between consecutive AS training pilots transmitted for each AE is $T_{\text{t}} = \alpha\, K\, T_{\text{s}}$.

To keep the *AS training phase* as short as possible, α is chosen as

$$\alpha = \left\lceil \frac{T_{\text{sw}}}{T_{\text{s}}} \right\rceil + 1 \tag{20}$$

where T_{sw} is the antenna switching time.

2) On receiving these AS training pilots, the receiver then:
   a) Obtains the preliminary channel gain estimates $\left\{ \tilde{h}_k [m] \mid m \in T_{\text{tr}}^k \right\}_{k=1}^{K}$ using (8).
   b) Performs channel prediction for each AE over the data time interval $\mathcal{I}_{\text{dt}}$ via (19)

$$\hat{h}_k^{\text{SP}} [m] = \boldsymbol{f}^T [m] \, \hat{\boldsymbol{\gamma}}_k = \sum_{i=0}^{D-1} \hat{\gamma}_{k,i} \, u_i [m] \tag{21}$$

   where $1 \le k \le K$, $m \in \mathcal{I}_{\text{dt}}$, and D is calculated from (15) (with L replacing J). Slepian prediction sequences $\{u_i [m] \mid m \in \mathcal{I}_{\text{dt}}\}_{i=0}^{D-1}$ are calculated from (18), and $\hat{\boldsymbol{\gamma}}_k \triangleq \left[\hat{\gamma}_{k,0}, \hat{\gamma}_{k,1}, \ldots, \hat{\gamma}_{k,D-1}\right]^T$ is of size $D \times 1$ and contains the basis expansion coefficients for AE k which are estimated via (16) $\big($with T_{tr}^k replacing $\mathcal{J}\big)$.
   c) Selects its receive AE $\hat{\imath}$ which maximizes the post-processing SNR over the data time interval $\mathcal{I}_{\text{dt}}$, which consists of N symbol durations, as

$$\hat{\imath} = \underset{1 \le k \le K}{\operatorname{argmax}} \sum_{m=M}^{M+N-1} \left| \hat{h}_k^{\text{SP}} [m] \right|^2 . \tag{22}$$

3) The single-antenna BS then sends out a length-N data packet which consists of $N - L'$ data symbols plus L' post-selection pilot symbols interleaved according to (9). Using the $L_{\text{tot}} = L + L'$ pilots, refined channel gain estimates $\left\{ \hat{h}_{\hat{\imath}}^{\text{SE}} [m] \mid m \in \mathcal{I}_{\text{dt}} \right\}$ are obtained by

$$\hat{\boldsymbol{h}}_{\hat{\imath}}^{\text{SE}} = \boldsymbol{U}' \, \hat{\boldsymbol{\gamma}}_{\hat{\imath}} = \sum_{i=0}^{D-1} \hat{\gamma}_{\hat{\imath},i} \, \boldsymbol{u}'_i \tag{23}$$

   where the $N \times 1$ vector $\hat{\boldsymbol{h}}_{\hat{\imath}}^{\text{SE}} \triangleq \left[\hat{h}_{\hat{\imath}}^{\text{SE}} [M], \hat{h}_{\hat{\imath}}^{\text{SE}} [M+1], \ldots, \hat{h}_{\hat{\imath}}^{\text{SE}} [M+N-1]\right]^T$, D is obtained from (15) (with L_{tot} replacing J), the $D \times 1$ vector $\hat{\boldsymbol{\gamma}}_{\hat{\imath}} \triangleq \left[\hat{\gamma}_{\hat{\imath},0}, \ldots, \hat{\gamma}_{\hat{\imath},D-1}\right]^T$ contains AE $\hat{\imath}$ basis expansion coefficients which are estimated using (16) (with $T_{\text{tot}}^{\hat{\imath}}$ replacing $\mathcal{J}$), $\boldsymbol{U}' \triangleq \left[\boldsymbol{u}'_0, \ldots, \boldsymbol{u}'_{D-1}\right]$ is the $N \times D$ *submatrix* of the *complete* $(M+N) \times D$ DPS sequences matrix $\boldsymbol{U}$. The vector $\boldsymbol{u}'_i \triangleq \left[u_i [M], u_i [M+1], \ldots, u_i [M+N-1]\right]^T$ is of size $N \times 1$.

We note that while other selection criteria may alternatively be used [20]; we consider the maximum total post-processing SNR criterion in (22).

Remark: In symbol-by-symbol AS, for each symbol an AE is selected. Since different AEs might be selected during the data transmission phase $\mathcal{I}_{\text{dt}}$, L' pilots should be sent to each AE in the data transmission phase so that refined channel gain estimates can be obtained for each AE. Thus, the number of pilots is now KL'. Note that we still have $\mathcal{I}_{\text{dt}} = \{M, M+1, \ldots, M+N-1\}$ since the switching time is less than the symbol duration. The above algorithm is converted into a symbol-by-symbol receive AS algorithm as follows: (i) In Step 2(c) the receiver then selects its receive AE, $\hat{\imath}_m$, for the data symbol at time m according to

$$\hat{\imath}_m = \underset{1 \le k \le K}{\operatorname{argmax}} \left| \hat{h}_k^{\text{SP}} [m] \right|^2 . \tag{24}$$

To denote this alternative AS strategy, symbol index m has been added to $\hat{\imath}$ in (24). (ii) In Step 3 the BS sends out a length-N data packet which consists of $N - KL'$ data symbols plus KL' pilots for the K AEs. Note that no AS is employed during the transmission of the KL' pilots. Thus, in total, $L_{\text{tot}} = L + L'$ pilot symbols are received by each AE. From these L_{tot} pilots, refined channel gain estimates $\left\{ \hat{h}_{\hat{\imath}_m}^{\text{SE}} [m] \mid m \in \mathcal{I}_{\text{dt}} \right\}$ are obtained using the Slepian basis estimator and used to decode data. To reduce overhead L' can be set to 1.

V. Symbol Error Probability (SEP) Analysis

In this section, we analyze the proposed receive AS algorithm from Section IV as well as the symbol-by-symbol receive AS, to evaluate the SEP of MPSK in time-varying channels.

A. Prediction and Estimation CSI Models

To derive closed-form expressions for the variances of the predicted/estimated channel gains and prediction/estimation errors, we first define the CSI uncertainty model for Slepian basis expansion estimation as

$$\hat{h}_k^{\text{SE}} [m] = h_k [m] + e_k^{\text{SE}} [m] , \qquad 1 \le k \le K, \; m \in \mathcal{I}_{\text{dt}} \tag{25}$$

where $\hat{h}_k^{\text{SE}} [m]$ is the estimated channel gain, $h_k [m]$ is the true channel gain, and $e_k^{\text{SE}} [m]$ is the estimation error. We assume the variables $h_k [m]$ and $e_k^{\text{SE}} [m]$ are uncorrelated. The true channel gain $h_k [m]$ is modeled as a zero-mean circularly symmetric complex Gaussian random variable (RV) with unit-variance. The true channel gain is correlated over time.

From (25), the variance of the channel gain estimate $\hat{h}_k^{\text{SE}} [m]$ can be expressed as

$$\sigma^2_{\hat{h}_k^{\text{SE}}} [m] = \sigma^2_{h_k} [m] + \sigma^2_{e_k^{\text{SE}}} [m] = 1 + \text{MSE}_k^{\text{SE}} [m] \tag{26}$$

where $\text{MSE}_k^{\text{SE}} [m]$ is the MSE per sample for the Slepian basis expansion estimator of AE k.

The MSE per sample of the Slepian basis expansion estimator for AE k takes the form [22]

$$\text{MSE}_k^{\text{SE}} [m] = \left(\text{bias}_k^{\text{SE}} [m] \right)^2 + \text{var}_k^{\text{SE}} [m] \tag{27}$$

where $\text{bias}_k^{\text{SE}} [m]$ and $\text{var}_k^{\text{SE}} [m]$ are the bias and variance terms, respectively. In (27), the squared bias term can be expressed as [22]

$$\left(\text{bias}_k^{\text{SE}} [m] \right)^2 = \int_{-\frac{1}{2}}^{+\frac{1}{2}} E_k^{\text{SE}} [m, \nu] \; S_h (\nu) \; \text{d}\nu \tag{28}$$

where $S_h (\nu)$ is the power spectral density (PSD) of the time-varying channel $\{h [m]\}$, and $E_k^{\text{SE}} [m, \nu]$ is the instantaneous error characteristic given by

$$E_k^{\text{SE}} [m, \nu] = \left| 1 - G_k^{\text{SE}} [m, \nu] \right|^2 . \tag{29}$$

Here, the instantaneous amplitude frequency response $G_k^{\text{SE}}[m,\nu]$ is given by

$$G_k^{\text{SE}}[m,\nu] = \boldsymbol{f}^T[m]\,\boldsymbol{G}_k^{-1}\sum_{l\in T_{\text{tot}}^k}\boldsymbol{f}^*[l]\,\exp\left(-j2\pi\nu\,(m-l)\right). \tag{30}$$

In (27), $\text{var}_k^{\text{SE}}[m]$ can be well approximated by [23]

$$\text{var}_k^{\text{SE}}[m] \approx N_0\,\boldsymbol{f}^\dagger[m]\,\boldsymbol{G}_k^{-1}\,\boldsymbol{f}[m]. \tag{31}$$

The CSI model for the Slepian basis expansion predictor can be obtained from (25)–(31) by replacing superscript $(\cdot)^{\text{SE}}$ by $(\cdot)^{\text{SP}}$ and T_{tot}^k by T_{tr}^k in (30).

B. SEP Analysis

1) SEP of Per-Packet Basis Selection: We now analyze the SEP of an MPSK symbol received at time m of a system which employs the per-packet basis receive AS algorithm in Sec. IV. Note that the predicted channel gains $\left\{\hat{h}_k^{\text{SP}}[m] \mid m\in\mathcal{I}_{\text{dt}}\right\}_{k=1}^K$ are used to select AE $\hat{\imath}$ to receive the length-N data packet, while the estimated channel gain $\hat{h}_{\hat{\imath}}^{\text{SE}}[m]$ is used to decode the received symbol at time m. The maximum-likelihood (ML) soft estimate for the symbol received by AE $\hat{\imath}$ at time m can be expressed as

$$\begin{aligned} r_{\hat{\imath}}[m] &= \left(\hat{h}_{\hat{\imath}}^{\text{SE}}[m]\right)^* y_{\hat{\imath}}[m] \\ &= \left|\hat{h}_{\hat{\imath}}^{\text{SE}}[m]\right|^2 d[m] - \left(\hat{h}_{\hat{\imath}}^{\text{SE}}[m]\right)^* d[m]\; e_{\hat{\imath}}^{\text{SE}}[m] \\ &\quad + \left(\hat{h}_{\hat{\imath}}^{\text{SE}}[m]\right)^* n_{\hat{\imath}}[m] \end{aligned} \tag{32}$$

where the last equality follows from substitution of (12), (13), and (25). Conditioned on $\hat{h}_{\hat{\imath}}^{\text{SE}}[m]$ and $d[m]$, $r_{\hat{\imath}}[m]$ in (32) is a complex Gaussian RV whose conditional mean $\mu_{r_{\hat{\imath}}}[m]$ and variance $\sigma_{r_{\hat{\imath}}}^2[m]$, as shown in the Appendix, are given by

$$\begin{aligned} \mu_{r_{\hat{\imath}}}[m] &\triangleq \mathbb{E}\left\{r_{\hat{\imath}}[m] \mid \hat{h}_{\hat{\imath}}^{\text{SE}}[m], d[m]\right\} \\ &= \left|\hat{h}_{\hat{\imath}}^{\text{SE}}[m]\right|^2 d[m]\;\zeta_{\hat{\imath}}^{\text{SE}}[m] \end{aligned} \tag{33}$$

$$\begin{aligned} \sigma_{r_{\hat{\imath}}}^2[m] &\triangleq \text{var}\left\{r_{\hat{\imath}}[m] \mid \hat{h}_{\hat{\imath}}^{\text{SE}}[m], d[m]\right\} \\ &= \left|\hat{h}_{\hat{\imath}}^{\text{SE}}[m]\right|^2 |d[m]|^2\left(1-\zeta_{\hat{\imath}}^{\text{SE}}[m]\right) \\ &\quad + N_0\left|\hat{h}_{\hat{\imath}}^{\text{SE}}[m]\right|^2 \end{aligned} \tag{34}$$

where $\mathbb{E}\{\cdot\}$ and $\text{var}\{\cdot\}$ denote statistical expectation and variance, respectively. $\zeta_{\hat{\imath}}^{\text{SE}}[m] \triangleq \frac{1}{1+\sigma^2_{e_{\hat{\imath}}^{\text{SE}}}[m]} = \frac{1}{1+\text{MSE}_{\hat{\imath}}^{\text{SE}}[m]}$, and the other symbols are defined in (13) and (26).

Conditioned on $\left\{\left\{\hat{h}_k^{\text{SP}}[m]\right\}_{m=M}^{M+N-1}\right\}_{k=1}^K$, $\hat{\imath}$, and $\hat{h}_{\hat{\imath}}^{\text{SE}}[m]$, the SEP of an MPSK symbol received at time m $\text{SEP}_m\left(\left\{\left\{\hat{h}_k^{\text{SP}}[m]\right\}_{m=M}^{M+N-1}\right\}_{k=1}^K, \hat{\imath}, \hat{h}_{\hat{\imath}}^{\text{SE}}[m]\right)$, which is denoted by $\text{SEP}_m(\varkappa)$, is [20], [24]

$$\begin{aligned} \text{SEP}_m(\varkappa) &= \frac{1}{\pi}\int_0^{\frac{\text{M}-1}{\text{M}}\pi}\exp\left(\frac{-\left|\mu_{r_{\hat{\imath}}}[m]\right|^2\sin^2\left(\frac{\pi}{\text{M}}\right)}{\sigma_{r_{\hat{\imath}}}^2[m]\,\sin^2(\theta)}\right)\mathrm{d}\theta \\ &= \frac{1}{\pi}\int_0^{\frac{\text{M}-1}{\text{M}}\pi}\exp\left(\frac{-\left|\hat{h}_{\hat{\imath}}^{\text{SE}}[m]\right|^2 b_{\hat{\imath}}^{\text{SE}}[m]}{\sin^2(\theta)}\right)\mathrm{d}\theta \end{aligned} \tag{35}$$

where $b_k^{\text{SE}}[m] \triangleq \frac{\left(\zeta_k^{\text{SE}}[m]\right)^2\sin^2\left(\frac{\pi}{\text{M}}\right)}{\left(1-\zeta_k^{\text{SE}}[m]\right)+\frac{1}{\eta}}$ and the last equality follows from substitution of (33) and (34). Note that the SEP expression above depends only $\hat{\imath}$ and $\hat{h}_{\hat{\imath}}^{\text{SE}}[m]$. We shall, therefore, denote (35) by $\text{SEP}_m\left(\hat{\imath}, \hat{h}_{\hat{\imath}}^{\text{SE}}[m]\right)$ henceforth.

Now averaging over the index $\hat{\imath}$ to get $\text{SEP}_m\left(\left\{\left\{\hat{h}_k^{\text{SP}}[m]\right\}_{m=M}^{M+N-1}\right\}_{k=1}^K, \left\{\hat{h}_k^{\text{SE}}[m]\right\}_{k=1}^K\right)$, which is denoted by $\text{SEP}_m(\Xi)$, yields

$$\begin{aligned} \text{SEP}_m(\Xi) &= \sum_{k=1}^K \Pr\left(\hat{\imath}=k \,\middle|\, \left\{\left\{\hat{h}_k^{\text{SP}}[m]\right\}_{m=M}^{M+N-1}\right\}_{k=1}^K\right) \\ &\quad \times\text{SEP}_m\left(\hat{\imath}=k, \hat{h}_{\hat{\imath}}^{\text{SE}}[m]\right) \\ &= \frac{1}{\pi}\sum_{k=1}^K\left(\prod_{\substack{l=1\\l\neq k}}^K \Pr\left(\sum_{m=M}^{M+N-1}\left|\hat{h}_l^{\text{SP}}[m]\right|^2 < \right.\right. \\ &\quad \left.\sum_{m=M}^{M+N-1}\left|\hat{h}_k^{\text{SP}}[m]\right|^2 \;\middle|\; \left\{\left\{\hat{h}_k^{\text{SP}}[m]\right\}_{m=M}^{M+N-1}\right\}_{k=1}^K\right)\Bigg) \\ &\quad \times\int_0^{\frac{\text{M}-1}{\text{M}}\pi}\exp\left(\frac{-\left|\hat{h}_k^{\text{SE}}[m]\right|^2 b_k^{\text{SE}}[m]}{\sin^2(\theta)}\right)\mathrm{d}\theta. \end{aligned} \tag{36}$$

After averaging over fading (i.e., Ξ), the SEP as a function of the SNR per branch $\eta = \frac{E_{\text{s}}}{N_0}$ is

$$\begin{aligned} \text{SEP}_m(\eta) &= \frac{1}{\pi}\sum_{k=1}^K\int_0^{\frac{\text{M}-1}{\text{M}}\pi}\int_0^\infty\int_0^\infty\exp\left(\frac{-x'\,b_k^{\text{SE}}[m]}{\sin^2(\theta)}\right) \\ &\quad \times f_{X_k',Y_k'}(x',y')\prod_{\substack{l=1\\l\neq k}}^K F_{Y_l'}(y')\,\mathrm{d}x'\mathrm{d}y'\mathrm{d}\theta \end{aligned} \tag{37}$$

where $f_{X_k',Y_k'}(x',y')$ is the joint probability distribution of the exponentially distributed RV $X_k' \triangleq \left|\hat{h}_k^{\text{SE}}[m]\right|^2$ and RV $Y_k' \triangleq \sum_{m=M}^{M+N-1}\left|\hat{h}_k^{\text{SP}}[m]\right|^2$. Thus, Y_k' is the sum of correlated exponentially distributed RVs, and $F_{Y_k'}(y')$ denotes its cumulative distribution function (CDF). Deriving a closed-form expression for $\text{SEP}_m(\eta)$ in (37) is analytically intractable since closed-form expressions for $f_{X_k',Y_k'}(x',y')$ and $F_{Y_k'}(y')$ do not exist. Therefore, Monte Carlo averaging techniques [25] are used to evaluate the fading-averaged SEP $\text{SEP}_m(\eta)$ from $\text{SEP}_m(\Xi)$.

We now derive the SEP of MPSK for a system that performs receive AS on a symbol-by-symbol basis. As shown in the next section, symbol-by-symbol AS is analytically tractable and provides insights for per-packet AS.

2) Symbol-By-Symbol AS SEP For MPSK: Receive AS is on an instantaneous symbol-by-symbol basis according to (24) with the channel gain estimate $\hat{h}_{i_m}^{\mathrm{SE}}[m]$ used to decode the MPSK symbol received at time m.

Theorem 1 The SEP of an MPSK symbol received at time m in a time-varying channel for a system with one transmit and K receive antennas employing selection criterion (24) with channel gain estimate $\hat{h}_{i_m}^{\mathrm{SE}}[m]$ to decode an MPSK symbol received at time m is given by

$$\begin{aligned} SEP'_m(\eta) &= \frac{1}{\pi}\sum_{k=1}^{K}\sum_{r=0}^{K-1}\sum_{\substack{l_0,\ldots,l_r=1\\ l_0=1,\, l_1\neq\ldots\neq l_r\neq k}}^{K}\frac{(-1)^r}{r!\left(4\sigma_{k,c_1}^2[m]\right)} \\ &\times\frac{1}{\sigma_{k,c_2}^2[m]\left(1-\left[\rho_{k,c_1c_2}^2[m]+\rho_{k,c_1s_2}^2[m]\right]\right)} \\ &\int_0^{\frac{M-1}{M}\pi}\int_0^{\infty}\int_0^{\infty}\exp\left(\frac{-x\,b_k^{SE}[m]}{\sin^2(\theta)}\right. \\ &-y\sum_{j=1}^{r}\zeta_{l_j}^{SP}[m]-\left[\frac{x}{\sigma_{k,c_1}^2[m]}+\frac{y}{\sigma_{k,c_2}^2[m]}\right] \\ &\left.\times\frac{1}{2\left(1-\left[\rho_{k,c_1c_2}^2[m]+\rho_{k,c_1s_2}^2[m]\right]\right)}\right) \\ &\times I_0\left(\frac{\sqrt{\rho_{k,c_1c_2}^2[m]+\rho_{k,c_1s_2}^2[m]}}{\left(1-\left[\rho_{k,c_1c_2}^2[m]+\rho_{k,c_1s_2}^2[m]\right]\right)}\right. \\ &\left.\times\frac{\sqrt{xy}}{\sigma_{k,c_1}[m]\,\sigma_{k,c_2}[m]}\right)\mathrm{d}x\,\mathrm{d}y\,\mathrm{d}\theta \end{aligned} \tag{38}$$

where the notation $\sum_{\substack{l_0,\ldots,l_r=1\\ l_0=1,\, l_1\neq\ldots\neq l_r\neq k}}^{K}$ compactly denotes $\sum_{l_0=1}^{1}\sum_{\substack{l_1=1\\ (l_1\neq k)}}^{K}\sum_{\substack{l_2=1\\ (l_2\neq k, l_2\neq l_1)}}^{K}\cdots\sum_{\substack{l_r=1\\ (l_r\neq k,\, l_r\neq l_1,\ldots,\, l_r\neq l_{r-1})}}^{K}$, $\zeta_{l_j}^{\mathrm{SP}}[m] \triangleq \frac{1}{\sigma^2_{\hat{h}_{l_j}^{\mathrm{SP}}[m]}} = \frac{1}{1+\sigma^2_{e_{l_j}^{\mathrm{SP}}[m]}} = \frac{1}{1+\mathrm{MSE}_{l_j}^{\mathrm{SP}}}$, $b_k^{\mathrm{SE}}[m] \triangleq \frac{\left(\zeta_k^{\mathrm{SE}}[m]\right)^2\sin^2\left(\frac{\pi}{M}\right)}{\left(1-\zeta_k^{\mathrm{SE}}[m]\right)+\frac{1}{\eta}}$, and $I_0(\cdot)$ is the zeroth-order modified Bessel function of the first kind. In (38), $\rho_{k,c_1c_2}[m]$ and $\rho_{k,c_1s_2}[m]$ denote the correlation coefficients of $(X_{k,c_1}[m], X_{k,c_2}[m])$ and $(X_{k,c_1}[m], X_{k,s_2}[m])$, respectively, where $X_k \triangleq \left|\hat{h}_k^{\mathrm{SE}}[m]\right|^2 = X_{k,c_1}[m] + jX_{k,s_1}[m]$ and $Y_k \triangleq \left|\hat{h}_k^{\mathrm{SP}}[m]\right|^2 = X_{k,c_2}[m] + jX_{k,s_2}[m]$, and $(X_{k,c_1}[m], X_{k,s_1}[m])$ and $(X_{k,c_2}[m], X_{k,s_2}[m])$ are i.i.d. zero-mean Gaussian RVs with variances $\sigma_{k,c_1}^2[m] = \sigma_{k,s_1}^2[m]$ and $\sigma_{k,c_2}^2[m] = \sigma_{k,s_2}^2[m]$, respectively.

Proof: The proof is given in the Appendix. ■

VI. Simulations

We now present numerical results to gain further insight into the previous analysis and study performance over time-varying channels. In the sequel, a system with one transmit and one receive antenna is denoted as 1×1, while a system with one transmit and K receive antennas out of which only one is selected is denoted as $1\times(1,K)$. Unless otherwise stated, a $1\times(1,K)$ system is simulated with the following parameters: (i) symbol duration $T_{\mathrm{s}} = 20.57\ \mu$s chosen according to [23], (ii) packet size $N = 40$ symbols, (iii) packet duration of 0.8228 ms, (iv) user velocity $v_{\max} = 100$ km/h $= 27.8$ m/s, (v) carrier frequency $f_{\mathrm{c}} = 2$ GHz, (vi) normalized Doppler bandwidth $\nu_{\max} = 3.8\times10^{-3}$, (vii) symmetric spectral support $\mathcal{W} = (-\nu_{\max},\ \nu_{\max})$, (viii) MPSK modulation with Gray labeling, and (ix) channel gains generated assuming plane-wave propagation [26], i.e.,

$$h[m] = \sum_{p=0}^{P-1} a_p\,\exp(j2\pi\nu_p m) \tag{39}$$

where the number of propagation paths is set to $P = 30$, the normalized Doppler shift per path $\nu_p = \nu_{\max}\cos\alpha_p$, where path angles α_p are uniformly distributed over $[-\pi\ \pi)$, the path weights are $a_p = \frac{1}{\sqrt{P}}\exp(j\psi_p)$, and ψ_p is uniformly distributed over $[-\pi\ \pi)$. We note that the random path parameters a_p and ν_p are assumed to be constant over an AS cycle time interval $\mathcal{I}_{\mathrm{cycle}} = \{0,1,\ldots,M+N-1\}$ but change independently from cycle to cycle. The covariance function of $\{h[m]\}$ converges to $R_h[\Delta m] = J_0(2\pi\nu_{\max}\Delta m)$ for $P\to\infty$, where $J_0(\cdot)$ is the zeroth order Bessel function of the first kind [22]. The channel model in (39) is also suitable for the evaluation of channel prediction algorithms [22].

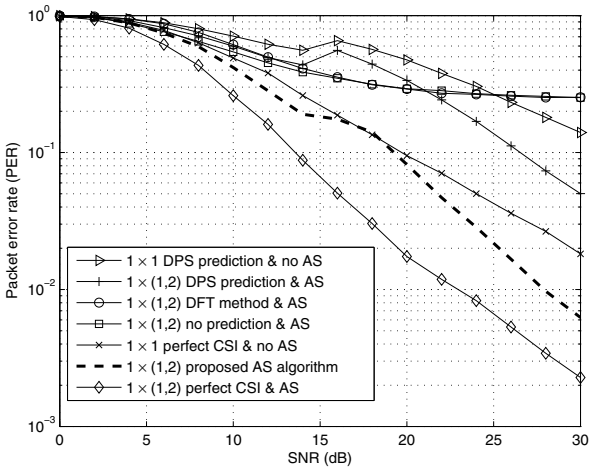

Fig. 3. PER performance of the proposed AS algorithm for a $1\times(1,2)$ system. (4PSK, data packet length $N = 40$, training pilots $L = 2$, post-selection pilots $L' = 2$, and $T_p = 3\,T_s$).

Figs. 3 and 4 show the PER of the proposed receive AS algorithm as a function of average SNR for $1\times(1,2)$ and $1\times(1,4)$ systems, respectively. For comparison, we also show the PER performance of (i) a 1×1 system with perfect CSI and no AS, (ii) a 1×1 system employing Slepian basis expansion channel prediction and no AS, (iii) $1\times(1,2)$ and $1\times(1,4)$ systems employing discrete Fourier transform (DFT) basis expansion channel prediction and AS according to the maximum total post-processing SNR selection criterion, as

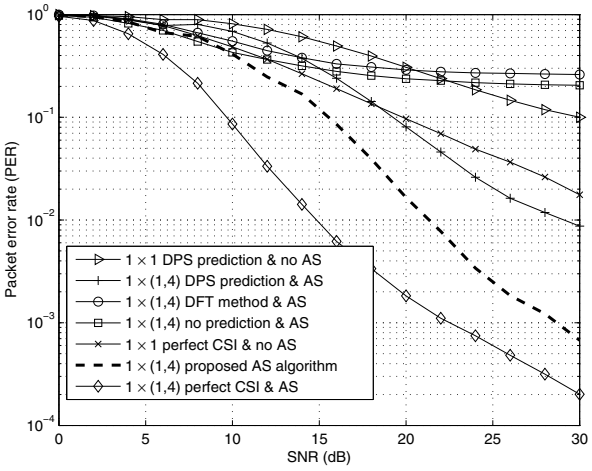

Fig. 4. PER performance of the proposed AS algorithm for a $1 \times (1,4)$ system. (4PSK, data packet length $N = 40$, training pilots $L = 2$, post-selection pilots $L' = 2$, and $T_p = 3\,T_s$).

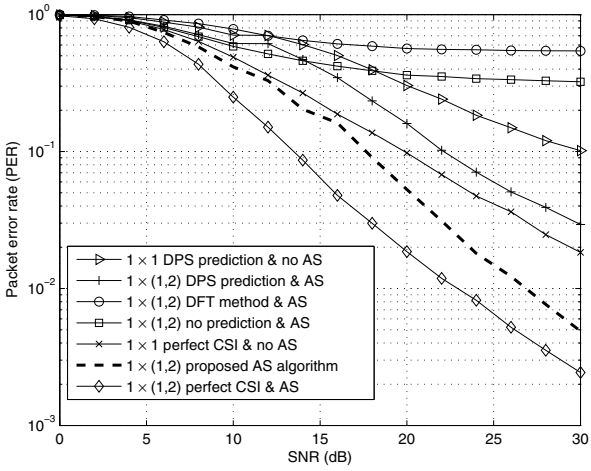

Fig. 5. PER performance of the proposed AS algorithm for a $1 \times (1,2)$ system. (4PSK, data packet length $N = 40$, training pilots $L = 3$, post-selection pilots $L' = 2$, and $T_p = 3\,T_s$).

in (22). DFT channel estimation is used for data decoding, (iv) $1\times(1,2)$ and $1\times(1,4)$ systems employing AS without channel prediction. We note that the antenna with the highest channel gain estimate $\tilde{h}_k\,[m]$ in (8) is selected since no channel prediction is used, (v) $1\times(1,2)$ and $1\times(1,4)$ systems employing Slepian channel prediction and AS according to (22), with the predicted channel gains $\left\{\hat{h}_k^{\mathrm{SP}}\,[m]\mid m\in\mathcal{I}_{\mathrm{dt}}\right\}$ used not only for selection but also data decoding, (vi) $1\times(1,2)$ and $1\times(1,4)$ systems employing the AS algorithm proposed in Sec. IV. Now the predicted channel gains are used for AE selection, while the refined channel gain estimates $\left\{\hat{h}_i^{\mathrm{SE}}\,[m]\mid m\in\mathcal{I}_{\mathrm{dt}}\right\}$ are used for decoding, and (vii) $1\times(1,2)$ and $1\times(1,4)$ systems with perfect CSI and employing AS according to (22) $\big($with $h_k\,[m]$ replacing $\hat{h}_k^{\mathrm{SP}}\,[m]\big)$. Inspection of Figs. 3 and 4 reveal that the $1\times(1,2)$ and $1\times(1,4)$ systems employing the proposed AS algorithm achieve SNR performance gains in excess of 3 dB and 9 dB over the 1×1 system with perfect CSI and no AS, respectively, at a PER equal to 10^{-2}. To highlight the importance of channel estimation, the performance of the same proposed $1\times(1,2)$ and $1\times(1,4)$ systems are about 5 dB and 6 dB worse than $1\times(1,2)$ and $1\times(1,4)$ systems employing AS with perfect CSI at the same PER of 10^{-2}, respectively. Also, error-floors exist at moderate to high SNR for the $1\times(1,2)$ and $1\times(1,4)$ systems employing AS either with DFT basis expansion or without channel prediction. In contrast, no error-floors arise with Slepian basis expansion.

Fig. 5 shows the PER of the proposed receive AS algorithm for a $1\times(1,2)$ system with $L=3$ AS training pilots rather than $L=2$ as in Fig. 3. Comparison of Figs. 3 and 5 confirms an SNR performance gain of about 1 dB at a PER $=10^{-2}$ due to the addition of one AS training pilot.

The analytical and simulation results for the sample mean of the Slepian estimator and predictor for AE k denoted by $\mathrm{MSE}_{k,N}^{\mathrm{SE}} \triangleq \frac{1}{N}\sum_{m=M}^{M+N-1}\mathrm{MSE}_k^{\mathrm{SE}}\,[m]$ and $\mathrm{MSE}_{k,N}^{\mathrm{SP}} \triangleq \frac{1}{N}\sum_{m=M}^{M+N-1}\mathrm{MSE}_k^{\mathrm{SP}}\,[m]$, respectively, are depicted in Fig. 6.

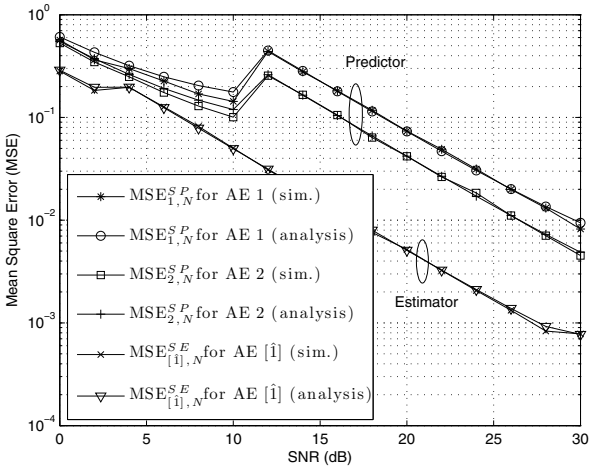

Fig. 6. Sample mean MSE_N of the basis expansion predictor and estimator for a $1\times(1,2)$ system. (Prediction/Estimation horizon $N=15$, training pilots $L=2$, post-selection pilots $L'=2$, and $T_p=5\,T_s$).

The sample mean is plotted for a $1\times(1,2)$ system with a packet length $N=15$, $L=2$ training pilot symbols, $L'=2$ post-selection pilot symbols, and $T_{\mathrm{p}}=5\,T_{\mathrm{s}}$. That is, AS training symbols for AE 1 and AE 2 are received at time indices $T_{\mathrm{tr}}^1=\{0,10\}$ and $T_{\mathrm{tr}}^2=\{5,15\}$, respectively. To evaluate the MSE per sample $\mathrm{MSE}_k^{\mathrm{SE}}\,[m]$ and $\mathrm{MSE}_k^{\mathrm{SP}}\,[m]$, given in Sec. V-A, we use Clarke's spectrum:

$$S_h\,(\nu)=\begin{cases}\frac{1}{\pi\nu_{\max}\sqrt{1-\left(\frac{\nu}{\nu_{\max}}\right)^2}} & |\nu|<\nu_{\max},\\ 0 & \text{otherwise.}\end{cases} \tag{40}$$

It can be observed that: (i) there is a very good match between the analytical and simulation results, (ii) the sample mean of the estimator is less than the sample mean of the predictor, (iii) the sample mean $\mathrm{MSE}_{2,N}^{\mathrm{SP}}$ of AE 2 is slightly less than the sample mean $\mathrm{MSE}_{1,N}^{\mathrm{SP}}$ of AE 1. This is expected since the AS training pilots for AE 2 are received closer in time to the prediction horizon $\mathcal{I}_{\mathrm{dt}}=\{20,21,\ldots,34\}$ than the AS training

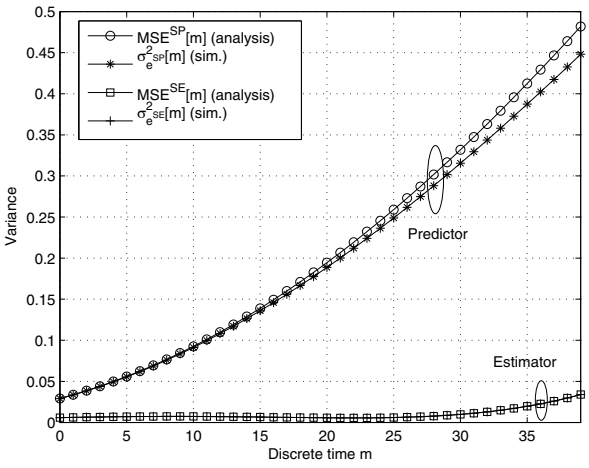

Fig. 7. Comparison of the simulated and calculated expressions for the basis expansion error variance for a 1×1 system at an average SNR $\eta = 20$ dB. (Prediction/Estimation horizon $N = 40$, training pilots $L = 2$, post-selection pilots $L' = 2$, and $T_p = 5\,T_s$).

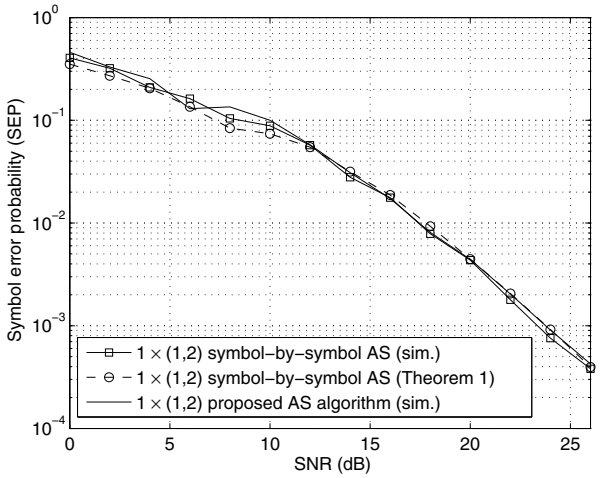

Fig. 8. SEP for the 20-*th* 4PSK data symbol as a function of the average SNR for a $1 \times (1, 2)$ system. (Data packet length $N = 40$, training pilots $L = 2$, post-selection pilots $L' = 2$, and $T_p = 5T_s$).

symbols for AE 1, and (iv) there are upward transitions in the estimation and prediction MSE curves which occur in the $2-4$ and $10 - 12$ dB ranges, respectively, which are the result of an increase of the subspace dimension D in (15). In addition, they indicate that D is suboptimal in these intervals.

Fig. 7 compares the simulated and analytically obtained variances of the estimation and prediction errors in Sec. V-A. It can be observed that: (i) these variances are close to each other, and (ii) not surprisingly, the MSE per sample of the predicted $\mathrm{MSE}^{\mathrm{SP}}[m]$, in contrast to the MSE per sample of the estimated $\mathrm{MSE}^{\mathrm{SE}}[m]$, increases with the prediction horizon, which is consistent with the behavior of typical prediction algorithms.

Fig. 8 shows the SEP of the 20-*th* 4PSK symbol as a function of average SNR for $1 \times (1, 2)$ systems employing the proposed receive AS algorithm and the symbol-by-symbol instantaneous receive AS scheme, which is analyzed in *Theorem 1*. It can be observed that the curves are close to each other. Since the SEP behaviour might be slightly different for the $N = 40$ different symbols of the data packet, we plot the SEP for the first 4PSK symbol in Fig. 9. A gap can be observed between the curves at moderate to high SNRs since channel prediction for the first symbol is much better than channel prediction for the 20-*th* symbol, which clearly affects the selection decision and, thus, the SEP. Similarly, there is a slight upward shift of the proposed AS scheme's SEP curve in Fig. 9, due to the fact that the first symbol is located far from the post-selection pilots $\mathcal{P} = \{11, 31\}$. We also observe from Figs. 8 and 9 and from other simulations (not included) that the SEP of the first few symbols in a packet for a system which uses symbol-by-symbol instantaneous receive AS is lower than that of the AS algorithm proposed in Sec. IV, while the SEPs of remaining symbols are close to one another.

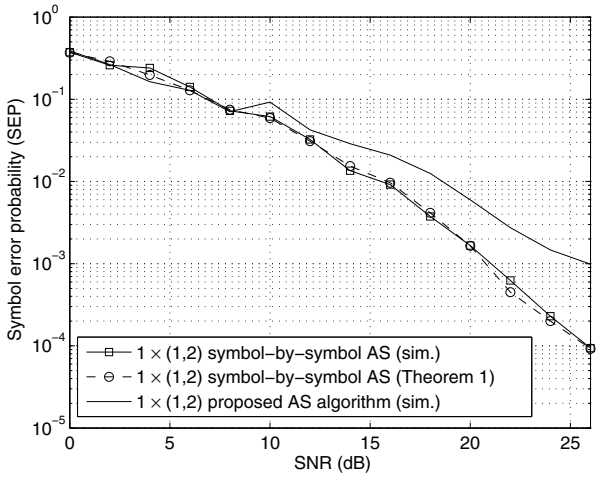

Fig. 9. SEP for the first 4PSK data symbol as a function of the average SNR for a $1 \times (1, 2)$ system. (Data packet length $N = 40$, training pilots $L = 2$, post-selection pilots $L' = 2$, and $T_p = 5T_s$).

VII. Conclusions

The downlink of a cellular radio system consisting of a single-antenna base station transmitting to a K-antenna mobile station is considered, where only one receive antenna is selected. By explicitly accounting for practical constraints imposed by next-generation wireless standards such as training and packet reception for antenna selection (AS), a single receive AS method is proposed for time-varying channels using the low-complexity Slepian basis expansion channel predictor and estimator. Closed-form expressions are derived for the channel prediction and estimation error as well as the SEP of MPSK with receive AS. It is shown that, in spite of the aforementioned realistic limitations, the proposed AS scheme outperforms ideal conventional SISO systems with perfect channel knowledge and no AS at the receiver and conventional complex basis based estimation. Although the focus was on single carrier communication over time-varying frequency-flat channels, the proposed AS scheme may be extendible to OFDM systems. The extension to the case where subsets of more than one receive antenna are selected in time-varying

frequency-selective channels remains as an important topic for future research.

APPENDIX

A. Derivation of the Conditional Mean and Variance

If A and B are zero-mean jointly complex Gaussian, then [20], [21]

$$\mathbb{E}\left\{A \,\middle|\, B\right\} = \mathbb{E}\left\{A\,B^*\right\}\left(\mathbb{E}\left\{B\,B^*\right\}\right)^{-1} B \tag{41}$$

$$\mathrm{var}\left\{A \,\middle|\, B\right\} = \mathrm{var}\left\{A\right\} - \mathbb{E}\left\{AB^*\right\}\left(\mathbb{E}\left\{BB^*\right\}\right)^{-1}\mathbb{E}\left\{BA^*\right\}. \tag{42}$$

From (41), it follows that $\mathbb{E}\left\{e_{\hat{\imath}}^{\mathrm{SE}}[m] \mid \hat{h}_{\hat{\imath}}^{\mathrm{SE}}[m]\right\} = \frac{\sigma^2_{e_{\hat{\imath}}^{\mathrm{SE}}}[m]}{1+\sigma^2_{e_{\hat{\imath}}^{\mathrm{SE}}}[m]}\hat{h}_{\hat{\imath}}^{\mathrm{SE}}[m]$ and $\mathbb{E}\left\{n_{\hat{\imath}}[m] \mid \hat{h}_{\hat{\imath}}^{\mathrm{SE}}[m]\right\} = 0$. Substituting and simplifying yields the desired conditional mean result in (33). Similarly, from (42) we get that $\mathrm{var}\left\{e_{\hat{\imath}}^{\mathrm{SE}}[m] \mid \hat{h}_{\hat{\imath}}^{\mathrm{SE}}[m]\right\} = \frac{\sigma^2_{e_{\hat{\imath}}^{\mathrm{SE}}}[m]}{1+\sigma^2_{e_{\hat{\imath}}^{\mathrm{SE}}}[m]}$ and $\mathrm{var}\left\{n_{\hat{\imath}}[m] \mid \hat{h}_{\hat{\imath}}^{\mathrm{SE}}[m]\right\} = N_0$. Substituting and simplifying yields the conditional variance result in (34).

B. Proof of Theorem 1

From (32), the ML soft estimate for the symbol received by AE $\hat{\imath}_m$ at time m can be modified to

$$\begin{aligned} r_{\hat{\imath}_m}[m] &= \left|\hat{h}_{\hat{\imath}_m}^{\mathrm{SE}}[m]\right|^2 d[m] - \left(\hat{h}_{\hat{\imath}_m}^{\mathrm{SE}}[m]\right)^* d[m]\, e_{\hat{\imath}_m}^{\mathrm{SE}}[m] \\ &\quad + \left(\hat{h}_{\hat{\imath}_m}^{\mathrm{SE}}[m]\right)^* n_{\hat{\imath}_m}[m]. \end{aligned} \tag{43}$$

Conditioned on $\hat{h}_{\hat{\imath}_m}^{\mathrm{SE}}[m]$ and $d[m]$, $r_{\hat{\imath}_m}[m]$ in (43) is a complex Gaussian RV whose conditional mean $\mu_{r_{\hat{\imath}_m}}[m]$ and variance $\sigma^2_{r_{\hat{\imath}_m}}[m]$ are given by

$$\mu_{r_{\hat{\imath}_m}}[m] = \left|\hat{h}_{\hat{\imath}_m}^{\mathrm{SE}}[m]\right|^2 d[m]\, \zeta_{\hat{\imath}_m}^{\mathrm{SE}}[m] \tag{44}$$

$$\begin{aligned} \sigma^2_{r_{\hat{\imath}_m}}[m] &= \left|\hat{h}_{\hat{\imath}_m}^{\mathrm{SE}}[m]\right|^2 |d[m]|^2 \left(1-\zeta_{\hat{\imath}_m}^{\mathrm{SE}}[m]\right) \\ &\quad + N_0 \left|\hat{h}_{\hat{\imath}_m}^{\mathrm{SE}}[m]\right|^2 \end{aligned} \tag{45}$$

where $\zeta_{\hat{\imath}_m}^{\mathrm{SE}}[m] \triangleq \frac{1}{1+\sigma^2_{e_{\hat{\imath}_m}^{\mathrm{SE}}}[m]} = \frac{1}{1+\mathrm{MSE}_{\hat{\imath}_m}^{\mathrm{SE}}}$.

Conditioned on $\left\{\hat{h}_k^{\mathrm{SP}}[m]\right\}_{k=1}^K$, $\hat{\imath}_m$, and $\hat{h}_{\hat{\imath}_m}^{\mathrm{SE}}[m]$, the SEP of an MPSK symbol received at time m $\mathrm{SEP}'_m\left(\left\{\hat{h}_k^{\mathrm{SP}}[m]\right\}_{k=1}^K, \hat{\imath}_m, \hat{h}_{\hat{\imath}_m}^{\mathrm{SE}}[m]\right)$, which is denoted by $\mathrm{SEP}'_m(\varkappa)$, is [20]

$$\begin{aligned} \mathrm{SEP}'_m(\varkappa) &= \frac{1}{\pi}\int_0^{\frac{\mathrm{M}-1}{\mathrm{M}}\pi} \exp\left(\frac{-\left|\mu_{r_{\hat{\imath}_m}}[m]\right|^2 \sin^2\left(\frac{\pi}{\mathrm{M}}\right)}{\sigma^2_{r_{\hat{\imath}_m}}[m]\,\sin^2(\theta)}\right)\mathrm{d}\theta \\ &= \frac{1}{\pi}\int_0^{\frac{\mathrm{M}-1}{\mathrm{M}}\pi} \exp\left(\frac{-\left|\hat{h}_{\hat{\imath}_m}^{\mathrm{SE}}[m]\right|^2 b_{\hat{\imath}_m}^{\mathrm{SE}}[m]}{\sin^2(\theta)}\right)\mathrm{d}\theta \end{aligned} \tag{46}$$

where $b_k^{\mathrm{SE}}[m] \triangleq \frac{\left(\zeta_k^{\mathrm{SE}}[m]\right)^2 \sin^2\left(\frac{\pi}{\mathrm{M}}\right)}{\left(1-\zeta_k^{\mathrm{SE}}[m]\right)+\frac{1}{\eta}}$, and the last equality follows from substituting (44) and (45). Note that the SEP expression above depends only on $\hat{\imath}_m$ and $\hat{h}_{\hat{\imath}_m}^{\mathrm{SE}}[m]$. Therefore, we shall denote it by $\mathrm{SEP}'_m\left(\hat{\imath}_m, \hat{h}_{\hat{\imath}_m}^{\mathrm{SE}}[m]\right)$ henceforth.

Now averaging over the index $\hat{\imath}_m$ to get $\mathrm{SEP}'_m\left(\left\{\hat{h}_k^{\mathrm{SP}}[m]\right\}_{k=1}^K, \left\{\hat{h}_k^{\mathrm{SE}}[m]\right\}_{k=1}^K\right)$, denoted for brevity by $\mathrm{SEP}'_m(\Xi)$, yields

$$\begin{aligned} \mathrm{SEP}'_m(\Xi) &= \sum_{k=1}^K \Pr\left(\hat{\imath}_m = k \,\middle|\, \left\{\hat{h}_k^{\mathrm{SP}}[m]\right\}_{k=1}^K\right) \\ &\quad \times \mathrm{SEP}'_m\left(\hat{\imath}_m = k, \hat{h}_{\hat{\imath}_m}^{\mathrm{SE}}[m]\right) \\ &= \frac{1}{\pi}\sum_{k=1}^K \left(\prod_{\substack{l=1\\ l\neq k}}^K \Pr\left(\left|\hat{h}_l^{\mathrm{SP}}[m]\right|^2 < \left|\hat{h}_k^{\mathrm{SP}}[m]\right|^2 \right.\right. \\ &\quad \left.\left. \,\middle|\, \left\{\hat{h}_k^{\mathrm{SP}}[m]\right\}_{k=1}^K\right)\right) \\ &\quad \times \int_0^{\frac{\mathrm{M}-1}{\mathrm{M}}\pi} \exp\left(\frac{-\left|\hat{h}_k^{\mathrm{SE}}[m]\right|^2 b_k^{\mathrm{SE}}[m]}{\sin^2(\theta)}\right)\mathrm{d}\theta. \end{aligned} \tag{47}$$

The expression for the SEP, when averaging over fading (i.e., Ξ), becomes

$$\begin{aligned} \mathrm{SEP}'_m(\eta) &= \frac{1}{\pi}\sum_{k=1}^K \int_0^{\frac{\mathrm{M}-1}{\mathrm{M}}\pi}\int_0^\infty\int_0^\infty \exp\left(\frac{-x\, b_k^{\mathrm{SE}}[m]}{\sin^2(\theta)}\right) \\ &\quad \times f_{X_k,Y_k}(x,y)\prod_{\substack{l=1\\ l\neq k}}^K F_{Y_l}(y)\,\mathrm{d}x\mathrm{d}y\mathrm{d}\theta \end{aligned} \tag{48}$$

where $f_{X_k,Y_k}(x,y)$ is the joint PDF of the two correlated exponentially distributed RVs $X_k \triangleq \left|\hat{h}_k^{\mathrm{SE}}[m]\right|^2 = X_{k,c_1}[m] + jX_{k,s_1}[m]$ and $Y_k \triangleq \left|\hat{h}_k^{\mathrm{SP}}[m]\right|^2 = X_{k,c_2}[m] + jX_{k,s_2}[m]$ given by [27]

$$\begin{aligned} f_{X_k,Y_k}(x,y) &= \frac{1}{4\,\sigma^2_{k,c_1}[m]\,\sigma^2_{k,c_2}[m]} \\ &\quad \times \frac{1}{\left(1-\left[\rho^2_{k,c_1c_2}[m]+\rho^2_{k,c_1s_2}[m]\right]\right)} \\ &\quad \times \exp\left(\left[\frac{x}{\sigma^2_{k,c_1}[m]}+\frac{y}{\sigma^2_{k,c_2}[m]}\right]\right. \\ &\quad \left.\times \frac{-1}{2\left(1-\left[\rho^2_{k,c_1c_2}[m]+\rho^2_{k,c_1s_2}[m]\right]\right)}\right) \\ &\quad \times I_0\left(\frac{\sqrt{\rho^2_{k,c_1c_2}[m]+\rho^2_{k,c_1s_2}[m]}}{\left(1-\left[\rho^2_{k,c_1c_2}[m]+\rho^2_{k,c_1s_2}[m]\right]\right)}\right. \\ &\quad \left.\times \frac{\sqrt{xy}}{\sigma_{k,c_1}[m]\,\sigma_{k,c_2}[m]}\right) \end{aligned} \tag{49}$$

where $x,\ y \geq 0$, $I_0(\cdot)$ is the zeroth-order modified Bessel function of the first kind, $(X_{k,c_1}[m],\ X_{k,s_2}[m])$ and $(X_{k,c_2}[m],\ X_{k,s_2}[m])$ are i.i.d. zero-mean Gaussian RVs with variances $\sigma^2_{k,c_1}[m] = \sigma^2_{k,s_1}[m]$ and

$\sigma^2_{k,c_2}[m] = \sigma^2_{k,s_2}[m]$, respectively. $\rho_{k,c_1c_2}[m]$ and $\rho_{k,c_1s_2}[m]$ are the correlation coefficients of $(X_{k,c_1}[m],\ X_{k,c_2}[m])$ and $(X_{k,c_1}[m],\ X_{k,s_2}[m])$, respectively, and lie in $(-1,1)$.

In (48), $F_{Y_l}(y)$ is the CDF of the exponentially distributed RV $Y_l \triangleq \left|\hat{h}_l^{\mathrm{SP}}[m]\right|^2$, and is given by

$$F_{Y_l}(y) = \begin{cases} 1-\exp\left(-\zeta_l^{\mathrm{SP}}[m]\ y\right), & y \geq 0 \\ 0, & y<0 \end{cases} \tag{50}$$

where the rate parameter is $\zeta_l^{\mathrm{SP}}[m] \triangleq \frac{1}{1+\sigma^2_{e_l^{\mathrm{SP}}}[m]} = \frac{1}{1+\mathrm{MSE}_l^{\mathrm{SP}}[m]}$.

Substituting (50) and (49) into (48) yields

$$\begin{aligned}
\mathrm{SEP}'_m(\eta) &= \frac{1}{\pi}\sum_{k=1}^{K}\int_0^{\frac{\mathtt{M}-1}{\mathtt{M}}\pi}\int_0^{\infty}\int_0^{\infty}\exp\left(\frac{-x\,b_k^{\mathrm{SE}}[m]}{\sin^2(\theta)}\right) \\
&\quad\times f_{X_k,Y_k}(x,y) \\
&\quad\times\prod_{\substack{l=1\\l\neq k}}^{K}\left(1-\exp\left(-\zeta_l^{\mathrm{SP}}[m]\ y\right)\right)\mathrm{d}x\,\mathrm{d}y\,\mathrm{d}\theta \\
&= \frac{1}{\pi}\sum_{k=1}^{K}\sum_{r=0}^{K-1}\sum_{\substack{l_0,\ldots,l_r=1\\ l_0=1,\,l_1\neq\ldots\neq l_r\neq k}}^{K}\frac{(-1)^r}{r!\left(4\sigma^2_{k,c_1}[m]\right)} \\
&\quad\times\frac{1}{\sigma^2_{k,c_2}[m]\left(1-\left[\rho^2_{k,c_1c_2}[m]+\rho^2_{k,c_1s_2}[m]\right]\right)} \\
&\quad\int_0^{\frac{\mathtt{M}-1}{\mathtt{M}}\pi}\int_0^{\infty}\int_0^{\infty}\exp\left(\frac{-x\,b_k^{\mathrm{SE}}[m]}{\sin^2(\theta)}\right. \\
&\quad\left.-y\sum_{j=1}^{r}\zeta_{l_j}^{\mathrm{SP}}[m]-\left[\frac{x}{\sigma^2_{k,c_1}[m]}+\frac{y}{\sigma^2_{k,c_2}[m]}\right]\right. \\
&\quad\left.\times\frac{1}{2\left(1-\left[\rho^2_{k,c_1c_2}[m]+\rho^2_{k,c_1s_2}[m]\right]\right)}\right) \\
&\quad\times I_0\left(\frac{\sqrt{\rho^2_{k,c_1c_2}[m]+\rho^2_{k,c_1s_2}[m]}}{\left(1-\left[\rho^2_{k,c_1c_2}[m]+\rho^2_{k,c_1s_2}[m]\right]\right)}\right. \\
&\quad\left.\times\frac{\sqrt{xy}}{\sigma_{k,c_1}[m]\,\sigma_{k,c_2}[m]}\right)\mathrm{d}x\,\mathrm{d}y\,\mathrm{d}\theta
\end{aligned} \tag{51}$$

where the identity $\prod_{\substack{l=1\\l\neq k}}^{K}\left(1-\exp\left(-\zeta_l^{\mathrm{SP}}[m]\ y\right)\right) = \sum_{r=0}^{K-1}\frac{(-1)^r}{r!}\sum_{\substack{l_0,\ldots,l_r=1\\ l_0=1,\,l_1\neq\ldots\neq l_r\neq k}}^{K}\exp\left(-y\sum_{j=1}^{r}\zeta_{l_j}^{\mathrm{SP}}[m]\right)$ is used in the last equality [20].

REFERENCES

[1] "Draft amendment to wireless LAN media access control (MAC) and physical layer (PHY) specifications: enhancements for higher throughput," Tech. Rep. P802.11n/D0.04, IEEE, Mar. 2006.

[2] "Technical specification group radio access network; evolved universal terrestrial radio access (E-UTRA); physical layer procedures (release 8)," Tech. Rep. 36.211 (v8.3.0), 3rd Generation Partnership Project (3GPP), 2008.

[3] N. B. Mehta, A. F. Molisch, J. Zhang, and E. Bala, "Antenna selection training in MIMO-OFDM/OFDMA cellular systems," in *Proc. 2007 IEEE CAMSAP*.

[4] A. F. Molisch and M. Z. Win, "MIMO systems with antenna selection," *IEEE Microw. Mag.*, vol. 5, pp. 46–56, Mar. 2004.

[5] S. Sanayei and A. Nosratinia, "Antenna selection in MIMO systems," *IEEE Commun. Mag.*, vol. 42, pp. 68–73, Oct. 2004.

[6] D. A. Gore and A. Paulraj, "MIMO antenna subset selection with space-time coding," *IEEE Trans. Signal Process.*, vol. 50, pp. 2580–2588, Oct. 2002.

[7] H. Mehrpouyan, S. D. Blostein, and E. C. Y. Tam, "Random antenna selection & antenna swapping combined with OSTBCs," in *Proc. 2007 IEEE ISSSE*.

[8] M. Z. Win and J. H. Winters, "Virtual branch analysis of symbol error probability for hybrid selection/maximal-ratio combining in Rayleigh fading," *IEEE Trans. Commun.*, vol. 49, pp. 1926–1934, Nov. 2001.

[9] A. Ghrayeb and T. M. Duman, "Performance analysis of MIMO systems with antenna selection over quasi-static fading channels," *IEEE Trans. Veh. Technol.*, vol. 52, pp. 281–288, Mar. 2003.

[10] A. F. Molisch, M. Z. Win, Y.-S. Choi, and J. H. Winters, "Capacity of MIMO systems with antenna selection," *IEEE Trans. Wireless Commun.*, vol. 4, pp. 1759–1772, July 2005.

[11] Z. Chen, J. Yuan, and B. Vucetic, "Analysis of transmit antenna selection/maximal-ratio combining in Rayleigh fading channels," *IEEE Trans. Veh. Technol.*, vol. 54, pp. 1312–1321, July 2005.

[12] Z. Xu, S. Sfar, and R. S. Blum, "Analysis of MIMO systems with receive antenna selection in spatially correlated Rayleigh fading channels," *IEEE Trans. Veh. Technol.*, vol. 58, pp. 251–262, Jan. 2009.

[13] Y. Jiang and M. K. Varanasi, "The RF-chain limited MIMO system–part I: optimum diversity-multiplexing tradeoff," *IEEE Trans. Wireless Commun.*, vol. 8, pp. 5238–5247, Oct. 2009.

[14] H. Zhang, A. F. Molisch, and J. Zhang, "Applying antenna selection in WLANs for achieving broadband multimedia communications," *IEEE Trans. Broadcast.*, vol. 52, pp. 475–482, Dec. 2006.

[15] W. Xie, S. Liu, D. Yoon, and J.-W. Chong, "Impacts of Gaussian error and Doppler spread on the performance of MIMO systems with antenna selection," in *Proc. 2006 WiCOM*.

[16] S. Han and C. Yang, "Performance analysis of MRT and transmit antenna selection with feedback delay and channel estimation error," in *Proc. 2007 IEEE WCNC*, pp. 1135–1139.

[17] W. M. Gifford, M. Z. Win, and M. Chiani, "Antenna subset diversity with non-ideal channel estimation," *IEEE Trans. Wireless Commun.*, vol. 7, pp. 1527–1539, May 2008.

[18] A. B. Narasimhamurthy and C. Tepedelenlioglu, "Antenna selection for MIMO-OFDM systems with channel estimation error," *IEEE Trans. Veh. Technol.*, vol. 58, pp. 2269–2278, June 2009.

[19] T. R. Ramya and S. Bhashyam, "Using delayed feedback for antenna selection in MIMO systems," *IEEE Trans. Wireless Commun.*, vol. 8, pp. 6059–6067, Dec. 2009.

[20] V. Kristem, N. B. Mehta, and A. F. Molisch, "Optimal receive antenna selection in time-varying fading channels with practical training constraints," *IEEE Trans. Commun.*, vol. 58, pp. 2023–2034, July 2010.

[21] ——, "Training and voids in receive antenna subset selection in time-varying channels," *IEEE Trans. Wireless Commun.*, vol. 10, pp. 1992–2003, June 2011.

[22] T. Zemen, C. F. Mecklenbräuker, F. Kaltenberger, and B. H. Fleury, "Minimum-energy band-limited predictor with dynamic subspace selection for time-variant flat-fading channels," *IEEE Trans. Signal Process.*, vol. 55, pp. 4534–4548, Sep. 2007.

[23] T. Zemen and C. F. Mecklenbräuker, "Time-variant channel estimation using discrete prolate spheroidal sequences," *IEEE Trans. Signal Process.*, vol. 53, pp. 3597–3607, Sep. 2005.

[24] M.-S. Alouini and A. Goldsmith, "A unified approach for calculating error rates of linearly modulated signals over generalized fading channels," *IEEE Trans. Commun.*, vol. 47, pp. 1324–1334, Sep. 1999.

[25] G. S. Fishman, *Monte Carlo: Concepts, Algorithms, and Applications*, 1st edition. Springer, 1996.

[26] R. H. Clarke, "A statistical theory of mobile-radio reception," *Bell Syst. Tech. J.*, vol. 47, pp. 957–1000, July-Aug. 1968.

[27] R. K. Mallik, "On multivariate Rayleigh and exponential distributions," *IEEE Trans. Inf. Theory*, vol. 49, pp. 1499–1515, June 2003.

Hassan A. Abou Saleh is currently pursuing his doctoral studies in electrical engineering at the Information Processing & Communications Laboratory (IPCL) at Queen's University, Kingston, Canada. He has been awarded a Natural Sciences and Engineering Research Council of Canada (NSERC) Postgraduate Scholarship (2009–2012). His areas of concentration are in wireless cutting-edge technologies and multiple antenna systems.

Andreas F. Molisch (S'89-M'95-SM'00-F'05) received the Dipl. Ing., Ph.D., and habilitation degrees from the Technical University of Vienna, Vienna, Austria, in 1990, 1994, and 1999, respectively. He subsequently was with AT&T (Bell) Laboratories Research (USA); Lund University, Lund, Sweden, and Mitsubishi Electric Research Labs (USA). He is now a Professor of electrical engineering with the University of Southern California, Los Angeles.

His current research interests are the measurement and modeling of mobile radio channels, ultra-wideband communications and localization, cooperative communications, multiple-input multiple-output systems, and wireless systems for healthcare. He has authored, coauthored, or edited four books (among them the textbook *Wireless Communications*, Wiley-IEEE Press), 14 book chapters, some 140 journal papers, and numerous conference contributions, as well as more than 70 patents and 60 standards contributions.

Dr. Molisch has been an Editor of a number of journals and special issues, General Chair, Technical Program Committee Chair, or Symposium Chair of multiple international conferences, as well as Chairman of various international standardization groups. He is a Fellow of the IET, an IEEE Distinguished Lecturer, and a member of the Austrian Academy of Sciences. He has received numerous awards, most recently the 2011 James Evans Avant-Garde award of the IEEE Vehicular Technology Society, the Donald Fink Prize of the IEEE, and the Eric Sumner Award of the IEEE.

Thomas Zemen (S'03-M'05-SM'10) was born in Mdling, Austria. He received the Dipl.-Ing. degree (with distinction) in electrical engineering from Vienna University of Technology in 1998 and the doctoral degree (with distinction) in 2004. From 1998 to 2003 he worked as hardware engineer and project manager for the radio communication devices department at Siemens Austria. Since October 2003 Thomas Zemen has been with FTW Forschungszentrum Telekommunikation Wien, he leads the department "Signal and Information Processing" since 2008. He is the speaker of the national research network for "Signal and Information Processing in Science and Engineering" funded by the Austrian Science Fund (FWF). His research interests include vehicular channel measurements and modelling, time-variant channel estimation, orthogonal frequency division multiplexing (OFDM), iterative multiple-input multiple-output (MIMO) receiver structures, cooperative communication systems and interference management. Dr. Zemen teaches as external lecturer at Vienna University of Technology and serves as editor for the IEEE TRANSACTIONS ON WIRELESS COMMUNICATIONS. He is the author or co-author of three books chapters and more than 80 journal papers and conference communications.

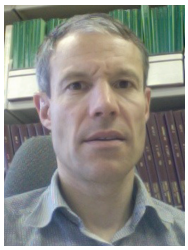

Steven D. Blostein (SM'83, M'88, SM'96) received his B.S. degree in Electrical Engineering from Cornell University, Ithaca, NY, in 1983, and the M.S. and Ph.D. degrees in Electrical and Computer Engineering from the University of Illinois, Urbana-Champaign, in 1985 and 1988, respectively. He has been on the faculty in the Department of Electrical and Computer Engineering Queen's University since 1988 and currently holds the position of Professor. From 2004-2009 he was Department Head. He has also been a consultant to industry and government in the areas of image compression, target tracking, radar imaging and wireless communications. He spent sabbatical leaves at Lockheed Martin Electronic Systems, McGill University and at Communications Research Centre in Ottawa. His current interests lie in the application of signal processing to problems in wireless communications systems, including synchronization, cooperative and network MIMO, and cross-layer optimization for multimedia transmission. He has been a member of the Samsung 4G Wireless Forum as well as an invited distinguished speaker. He served as Chair of IEEE Kingston Section (1994), Chair of the Biennial Symposium on Communications (2000,2006,2008), Associate Editor for IEEE TRANSACTIONS ON IMAGE PROCESSING (1996-2000), and Publications Chair for IEEE ICASSP 2004, and an Editor of IEEE TRANSACTIONS ON WIRELESS COMMUNICATIONS (2007-present). He has also served on Technical Program Committees for IEEE Communications Society conferences for many years. He is a registered Professional Engineer in Ontario and a Senior Member of IEEE.

Neelesh B. Mehta (S'98-M'01-SM'06) received his Bachelor of Technology degree in electronics and communications engineering from the Indian Institute of Technology (IIT), Madras in 1996, and his M.S. and Ph.D. degrees in electrical engineering from the California Institute of Technology, Pasadena, CA, USA in 1997 and 2001, respectively. He is now an Associate Professor in the Dept. of Electrical Communication Eng., Indian Institute of Science (IISc), Bangalore, India. Prior to joining IISc in 2007, he was a research scientist from in the Wireless Systems Research Group in AT&T Laboratories, Middletown, NJ, USA from 2001 to 2002, Broadcom Corp., Matawan, NJ, USA from 2002 to 2003, and Mitsubishi Electric Research Laboratories (MERL), Cambridge, MA, USA from 2003 to 2007.

His research includes work on link adaptation, multiple access protocols, WCDMA downlinks, cellular systems, MIMO and antenna selection, energy harvesting networks, and cooperative communications. He was also actively involved in the Radio Access Network (RAN1) standardization activities in 3GPP from 2003 to 2007. He has served on several TPCs. He was a TPC co-chair for the WISARD 2010 and 2011 workshops and tracks in NCC 2011, SPCOM 2010, VTC 2009 (Fall), and Chinacom 2008. He will serve as a TPC co-chair of the Wireless Communications Symposium of ICC 2013. He has co-authored 30 IEEE journal papers, 55 conference papers, and 3 book chapters, and is a co-inventor in 16 issued US patents. He was an Editor of the IEEE TRANSACTIONS ON WIRELESS COMMUNICATIONS from 2008 to 2011. He is now an Editor of IEEE WIRELESS COMMUNICATIONS LETTERS. He is currently serving as Director of Conference Publications in the Board of Governors of the IEEE Communications Society. He is also an executive committee member of the IEEE Bangalore Section and the Bangalore Chapter of the IEEE Signal Processing Society.